
NASA Technical Paper 1832

# Performance of Computer-Designed Small-Sized Four-Stage Depressed Collector for Operation of Dual-Mode Traveling Wave Tube

Peter Ramins and Thomas A. Fox



AUGUST 1981

NASA

NASA Technical Paper 1832

# Performance of Computer-Designed Small-Sized Four-Stage Depressed Collector for Operation of Dual-Mode Traveling Wave Tube

Peter Ramins and Thomas A. Fox
*Lewis Research Center*
*Cleveland, Ohio*

National Aeronautics
and Space Administration

**Scientific and Technical
Information Branch**

1981

## Summary

A computer-designed axisymmetric 2.4-centimeter-diameter four-stage depressed collector was evaluated in conjunction with an octave-bandwidth, dual-mode traveling wave tube (TWT). The TWT was operated over a wide range of conditions to simulate different applications. The collector performance was optimized (within the constraint of fixed collector geometry which was designed for operation of the TWT at saturation) over the range of TWT operating conditions covered.

For operation of the dual-mode TWT at saturation, average collector efficiencies of 81 ½ and 82 percent for the high and low modes, respectively, were obtained across an octave bandwidth, leading to a three-fold increase in the TWT overall efficiency.

For operation of the TWT in the linear, low distortion range, collector efficiencies of 87 to 92 percent were obtained, leading to TWT overall efficiencies as high as 35 percent. For operation of the dual-mode TWT over a 10 to 1 range in output power, overall efficiencies of 14 to 41 percent were obtained.


## Introduction

In a joint USAF–NASA program, the Lewis Research Center is conducting an efficiency improvement program on traveling wave tubes (TWT's) for use in electronic countermeasure (ECM) and communication systems by applying the multistage depressed collector (MDC) and spent beam refocusing techniques developed at Lewis (refs. 1 to 4). These techniques convert a large part of the kinetic power of the spent electron beam at the TWT output to useful electric power, substantially increasing the overall efficiency. This is of particular significance to airborne and space applications because the overall efficiency has a direct bearing on the size, weight, and complexity of the prime power, power conditioning, and heat rejection systems.

The refocusing system and MDC designs are produced by combining the analysis of the TWT, the refocusing system, and the MDC (ref. 5). Representative charges are tracked from the radiofrequency (rf) input of the TWT to their collection on the MDC electrodes.

This design procedure was used to design an axisymmetric 2.4-centimeter-diameter four-stage depressed collector[1] for an octave-bandwidth, periodic-permanent-magnet (PPM) focused, dual-mode TWT (Teledyne MEC model MTZ 7000). The collector geometric design (shown in fig. 1) was optimized for saturated operation of the TWT in the low (CW) mode with no consideration for other TWT applications.

The MDC and a refocusing system were added to the TWT and operated over a wide range of conditions to simulate the applications where:

(1) An octave bandwidth dual-mode TWT is pulsed between the low and high modes, both at saturation.

(2) A TWT is operated CW at saturation across an octave bandwidth.

(3) A 10:1 pulse-up capability in the output power is needed, and the lower power mode represents TWT operation well below saturation.

(4) The TWT must be operated at constant output power in the linear, low-distortion range (typically 3 dB or more below saturation).

The results of these tests are reported herein. The results of the TWT, refocusing system, and MDC analysis are reported in reference 6.

## Symbols[2]

| | |
|---|---|
| $B_z$ | axial magnetic field, T |
| $e$ | electronic charge |
| $I_B$ | true interception current in forward direction |
| $I_{body}$ | $I_B + I_S$ |
| $I_{En}$ | collector current to $n^{th}$ electrode |
| $I_{E0}$ | backstreaming current to undepressed collector electrode |
| $I_k$ | cathode current or beam current |
| $I_S$ | backstreaming current to TWT body |
| $P_{body}$ | (total rf losses in TWT) + (true beam interception losses) |
| $P'_{body}$ | $P_{body}$ + (all or part of backstreaming power) |

[1] Designed by J.A. Dayton of Lewis Research Center.

[2] See also figs. 2 and 3.

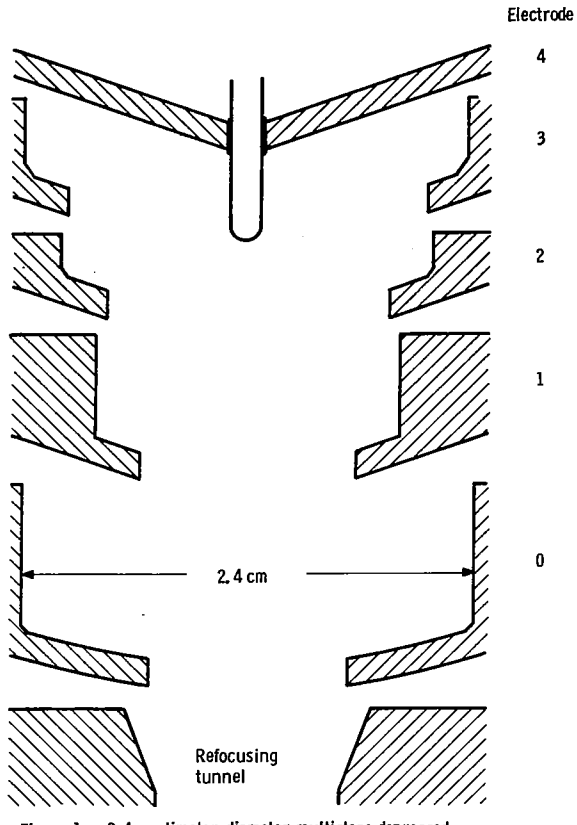


Figure 1. - 2.4-centimeter-diameter multistage depressed collector (MDC).

| | |
|---|---|
| $P_{coll}$ | total power in spent beam that enters MDC |
| $P_{fund}$ | radiofrequency output associated with fundamental frequency |
| $P_{hrm}$ | radiofrequency output resulting from harmonic frequencies |
| $P_{recovered}$ | defined in figure 2 |
| $P_{rf}$ | total rf output ($P_{fund} + P_{hrm}$) |
| $P_{therm}$ | $P_{rf} + P'_{body}$ + (total collector dissipation) |
| $P_{tot}$ | prime power, ($V_k I_k - P_{recovered}$) |
| $(r,\theta,z)$ | cylindrical coordinates |
| $\overline{V}$ | average potential of intercepted electrons |
| $V_k$ | cathode potential (always negative for work reported herein) |

## Experimental TWT and MDC Performance Evaluation

To obtain complete and accurate TWT and MDC performance evaluations, it is necessary to determine

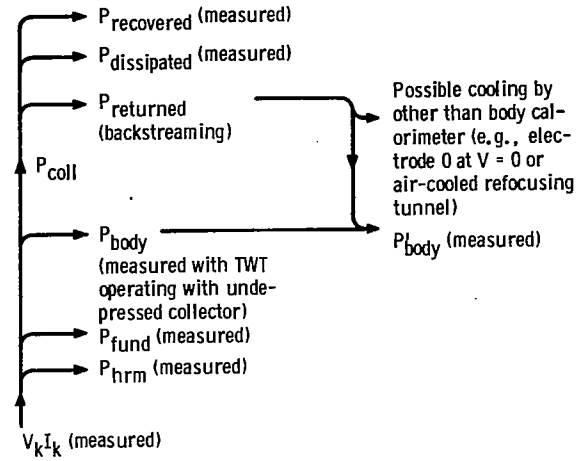


$P_{body}$ = (rf circuit losses) + (intercepted power in forward direction)

$P'_{body} = P_{body}$ + (all or part of backstreaming power)

$P_{coll} = V_k I_k - P_{rf} - P_{body}$

Collector efficiency = $P_{recovered}/P_{coll}$

(a) Power flow.

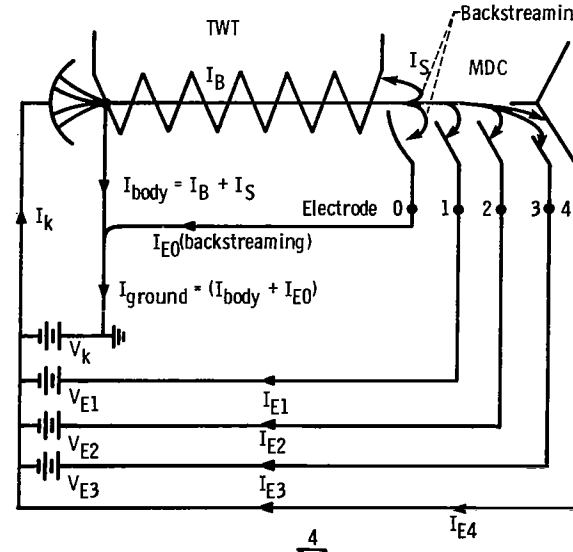


dc input power = $V_k(I_{ground}) + \sum_{n=1}^{4} V_{En} I_{En}$

$$P_{recovered} = \sum_{n=1}^{4} \left( \left| V_k - V_{En} \right| \right) (I_{En})$$

$P_{coll} = V_k I_k - P_{rf}$ - (circuit losses) - ($I_B \overline{V}$) where $e\overline{V}$ is average energy of intercepted electrons

$P_{coll} \neq V_k I_k - P_{rf}$ - (circuit losses) - ($I_{ground} V_k$)

(b) Electron flow.

Figure 2. - Flow diagrams for TWT with MDC.

the final power distribution in the system. This distribution is shown in figure 2 in the form of power-flow and electron-flow diagrams for a TWT with a depressed collector. Part of the initial beam power ($I_k V_k$) appears as measured radiofrequency (rf) output power at the fundamental and (possibly) harmonic frequencies, and part is dissipated by the TWT body as the sum of rf losses in the TWT and intercepted beam power in the forward direction. The rest of the beam power enters the collector. Part of this kinetic power is recovered as useful electric power, and part is dissipated as thermal power on the collector plates. Collector efficiency is defined as $P_{recovered}/P_{coll}$.

With a depressed collector, the possibility exists of backstreaming electrons ($I_S$ and $I_{E0}$ in fig. 2(b)) returning significant power to the TWT body. Since any backstreaming produced by the depressed collector must be accounted for in determining efficiency, this backstreaming power must be evaluated and charged against the depressed collector, or exaggerated collector efficiencies will result. A more complete discussion of this problem can be found in reference 7.

It should be noted that neither $P_{coll}$, $P_{body}$, nor true beam interception $I_B$ can be measured directly for a tube operated with an MDC. Without these measured values, the determination of MDC efficiencies requires certain assumptions that can significantly affect the computed collector performance:

(1) Assumption of the circuit losses (rf losses on the rf structure)

(2) Assumption of the true intercepted current in the forward direction

(3) Assumption of the average energy of the intercepted electrons.

With these assumptions $P_{coll}$ can be computed from the equation

$$P_{coll} = V_k I_k - (\text{circuit losses}) - (I_B \overline{V}) - P_{rf}$$

as shown in figure 2(b).

However, it has been our experience at Lewis that both the circuit losses and the true beam interception can vary widely, even between TWT's of identical design (ref. 8). Circuit losses at a given frequency can be strongly affected by reflections due to mismatches (individual TWT imperfections), and the TWT's are usually focused to meet system specifications, not to produce minimum beam-current interception.

The need for making any assumptions can be avoided entirely only by first operating the same TWT with a suitable thermally isolated undepressed collector. The power returned to the TWT body by backstreaming electrons (secondaries) from such a collector is negligible. The power flow diagram for a TWT with an undepressed collector is shown in figure 3. The power into the collector $P_{coll}$ can be measured directly, or alternatively, $P_{rf}$ and $P_{body}$ can be thermally measured and $P_{coll}$ computed from measured quantities. Since only the total body power $P_{body}$ is needed for the computation of $P_{coll}$, it can be seen that with this experimental approach the questions of circuit efficiency, true interception, and the average energy of the intercepted electrons are irrelevant.

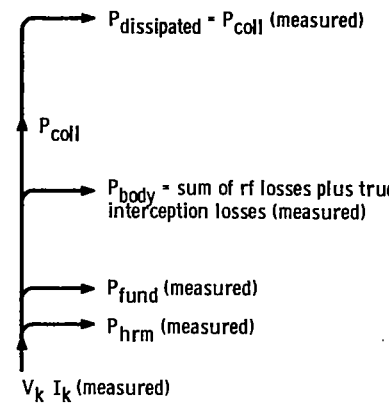


Figure 3. - Power flow diagram for TWT with undepressed collector.

## Experimental TWT

The Teledyne MEC model MTZ 7000 (TWT 103) as modified for use in this program and its performance characteristics are shown in figure 4. A refocusing system consisting of two coils has been added, and the TWT is mounted on a 25.4-centimeter (10-in.) ultrahigh-vacuum (UHV) flange. The UHV valve shown was designed to keep the TWT under vacuum during MDC installation and changes, facilitating startup and minimizing cathode activation problems (ref. 9).

This TWT was delivered with an undepressed thermally isolated water-cooled collector mounted on a matching 25.4-centimeter (10-in.) vacuum flange. This special collector was required for the bench test.

## Experimental Arrangement

### Bench Test

The purpose of the bench test was to document the performance of the TWT as delivered with an undepressed spent-beam collector so that TWT performance changes, if any, due to the MDC can be

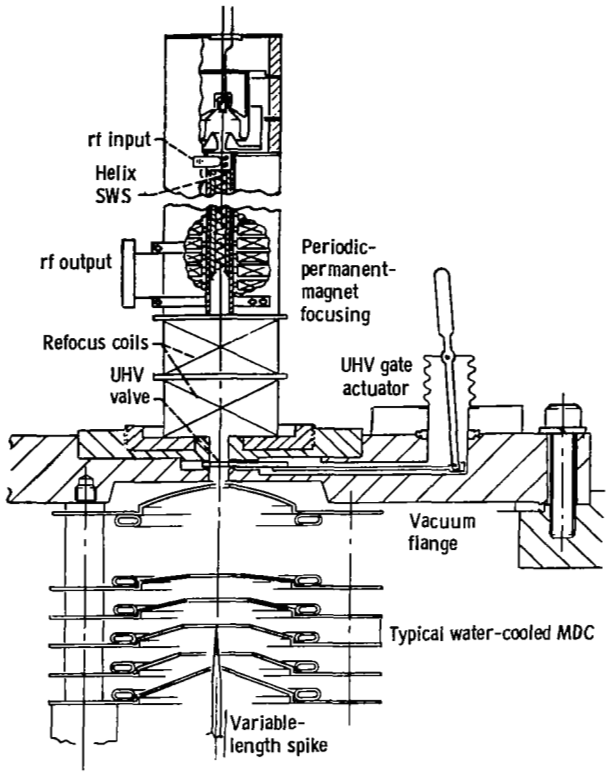


Figure 4. - Schematic of MEC TWT 103 with MDC. Frequency, 4.8 to 9.6 gigahertz; total maximum rf output, 500 watts in low mode and 820 watts in pulsed-up mode; cathode potential, 9950 volts; beam current, 0.38 ampere in low mode and 0.49 ampere in pulsed-up mode; duty cycle, 100 percent in low mode and 25 percent in pulsed-up mode.

determined and so that accurate MDC efficiency measurements could later be made. The rf load, TWT body, and collector are all thermally isolated and water cooled. Thermal power to each is measured by a combination of flowmeter and thermopile. Since the collector is undepressed, the power returned to the TWT by any backstreaming electrons is negligible. The measured $P_{body}$ is, therefore, the sum of the total rf losses in the TWT and the interception losses.

## Multistage Depressed Collector Test

In the MDC test setup (fig. 5) the TWT is mounted on a matching flange on a UHV system. The MDC is mounted directly on the UHV flange, which houses the TWT and vacuum valve. Each MDC electrode, including the undepressed electrode, is thermally and electrically isolated and is water cooled. The spent-beam power recovered by each MDC electrode, as well as the thermal (kinetic) power dissipated on each electrode, was measured. A vacuum feedthrough

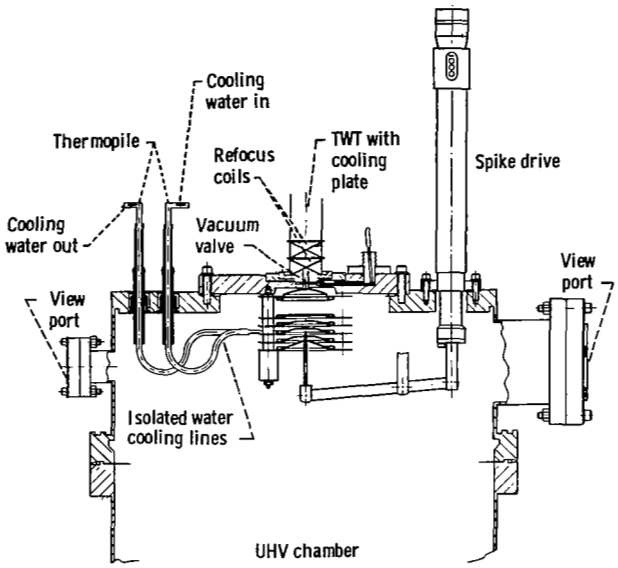


Figure 5. - Schematic of MDC measuring system.

drives a variable-length spike. Over its range of variability, the length of the spike significantly affects the electric-field distribution within the collector, and its optimum length can be established quickly and easily for each MDC configuration. Since the refocusing coils and pole pieces are outside the vacuum, they can be manipulated and moved over their designed range of variability while the TWT is operating. Together with variation of the refocusing coil currents, this enables the rapid optimization, within limits, of the refocusing field profile. Once established, this profile can be synthesized with a permanent-magnet refocusing system.

A typical experimental collector arrangement is shown in figure 5. This fully demountable mechanical design was chosen for experimental convenience. Separate water cooling and calorimetry of each collector electrode were chosen for diagnostic purposes and for the system's ability to provide information for the eventual thermal design of a conduction-cooled MDC.

A novel data acquisition system was used to optimize collector efficiency under various conditions. This system provides an analog real-time readout of the recovered power as any of the system variables are changed while the TWT is operating. These variables are the individual collector stage voltages, the refocusing coil currents, the polepiece locations, and the spike length.

Maximizing recovered power is identical to maximizing the MDC efficiency. Once the optimum combination of operating conditions is found, an automated system is used for actual data taking.

## Experimental Program and Results

### Traveling-Wave Tube Bench Test

The dual-mode TWT with an undepressed collector was operated at saturation across the octave bandwidth in both the low and high modes. In addition, at selected operating frequencies the TWT performance and fixed TWT losses were evaluated at rf powers as much as 12 decibels below saturated output power. The results are discussed in reference 10. Unless otherwise specifically noted, these measured values of $P_{body}$ were used for all subsequent computations of collector efficiency.

### Multistage Depressed Collector Test Conditions and Results

The four-stage depressed collector was added to the TWT, and the combination evaluated. The single MDC geometric design used in these tests was analytically optimized for saturated operation in the low mode. Within this constraint of fixed geometry (not optimum for a broad range of operating conditions) the MDC performance was optimized for the various operating conditions discussed previously by varying:

(1) The electrode voltages
(2) The refocusing system profile
(3) The MDC spike length

Data for the low and high modes were obtained at duty cycles of 100 and 25 percent, respectively. A coating of carbon black on electrodes 1 to 4 was used to suppress secondary electron emission from the MDC collecting surfaces.

The TWT was operated at times at higher beam currents than those used during the bench test. Since the voltage on the focus electrode (used to adjust $I_k$) has an effect on the body current, the true value of $P_{body}$ during these tests was unknown. The bench test measured values of $P_{body}$ are, nevertheless, believed to be accurate estimates since the interception of this TWT was very low (¾ to 1 ¼ percent) and the expected small decrease (observed on another model of this TWT) in $I_B$ would be offset by higher circuit losses. Collector efficiencies determined under these conditions are labeled as estimated collector efficiencies.

The overall efficiencies determined in these tests are based on the total rf power generated, since no attempt was made to measure separately the rf power generated at the fundamental and harmonic frequencies. To obtain approximate efficiencies based on $P_{fund}$, the overall efficiencies (both with and without the MDC) in the range of operating frequencies of 4.8 to 5.6 gigahertz should be multiplied by the following approximate factors (ref. 10):

| Frequency, GHz | Low mode | High mode |
|---|---|---|
| | $P_{fund}/P_{rf}$ | |
| 4.8 | 0.7 | 0.62 |
| 5.2 | 0.86 | 0.72 |
| 5.6 | 0.99 | 0.87 |

*Final energy balance of the TWT-MDC system.*—An example of the data obtained and the energy (power) balance established at a specific operating point is shown in table I. The currents, voltages, and powers have been rounded off after computation.

The total rf power generated, the TWT body losses, including any backstreaming to the TWT body, and the power dissipated in the MDC, including backstreaming to the undepressed electrode, are all thermally measured. Their sum is $P_{therm}$. The possibility exists, however, of some backstreaming electrons (part of $I_S$, but not measured separately) being collected in the air-cooled section of the refocusing tunnel. No attempt was made to measure the resulting thermal dissipation directly. Such backstreaming shows up as the difference between $P_{tot}$ and $P_{therm}$ (72 W for the example in table I).

*Dual-mode TWT-MDC performance at saturation.*—In order to evaluate the MDC performance when the TWT is pulsed between the high and low modes, a compromise optimization was performed. The TWT-MDC performance in both the low and high modes was then evaluated across an octave bandwidth for this fixed set of MDC and refocusing system operating conditions.

The results are shown in figures 6 and 7. A very significant improvement in the TWT overall efficiency was obtained for both modes. The average overall efficiency across the octave bandwidth was improved from 12 percent (without MDC) to 39 percent (with MDC) in the low mode and from 14 percent to 42 percent in the high mode. The average collector efficiencies were 81.9 and 81.4 for the low and high modes, respectively. The performance of the collector was found to be relatively constant for both modes and across the octave bandwidth in spite of substantial changes in the rf output power.

The distributions of currents to the various collector stages as a function of frequency are given in figure 8(a) for the low mode and figure 8(b) for the high mode. The dc input powers to the various collector stages as a function of frequency are shown in figure 9(a) for the low mode and figure 9(b) for the high mode. The maximum dc input power was 1.2



TABLE I. – RESULTS FOR TWT 103 WITH FIVE-STAGE COLLECTOR DEMONSTRATING FINAL ENERGY BALANCE AT A REPRESENTATIVE FREQUENCY

(a) Tube test conditions and results

| | |
|---|---|
| Frequency, GHz | 9.2 |
| $P_{in}$, mW | 180 |
| $P_{fund}$, W | 493 |
| $P_{hrm}$, W | 0 |
| Gain, dB | 34 |
| Duty cycle, percent | 100 |
| $V_k$, kV | 9.94 |
| $I_k$, mA | 380 |
| Beam power, W | 3777 |
| $P_{body}$, W | 121 |
| $P'_{body}$, W | 155 |
| $I_B$, mA | 4.4 |
| $I_S$, mA | 18.4 |

(b) MDC test conditions and results

| Collector electrode | Voltage,[a] kV | Current, mA | Power, W | |
|---|---|---|---|---|
| | | | Recovered | Dissipated |
| 0 | 0 | 5.4 | 0 | 40 |
| 1 | −5.73 | 143.3 | 821 | 136 |
| 2 | −7.09 | 51.8 | 367 | 80 |
| 3 | −9.07 | 155.8 | 1413 | 154 |
| 4 | −9.94 | 1.7 | 17 | 29 |
| Total | | | 2618 | 439 |

Collector efficiency, 82.8 percent
Overall efficiency, 42.5 percent
$P_{therm}$ = 1087
$P_{tot}$ = 1159

(c) Final energy balance

| | |
|---|---|
| Useful rf power, W | 493 |
| TWT body losses, W | 121 |
| Backstreaming to TWT body, W | 34 |
| Backstreaming to refocusing tunnel,[b] W | 72 |
| Backstreaming to undepressed collector, W | 40 |
| Collector (2 to 6) dissipation, W | 399 |
| Recovery power, W | 2618 |
| Total power | 3777 |

[a]With respect to ground potential.
[b]Computed from $(P_{tot} - P_{therm})$.

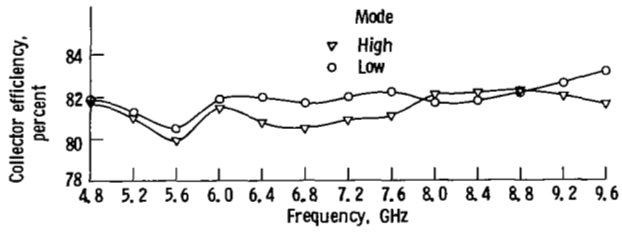


Figure 6. - Collector efficiency versus frequency at saturation.

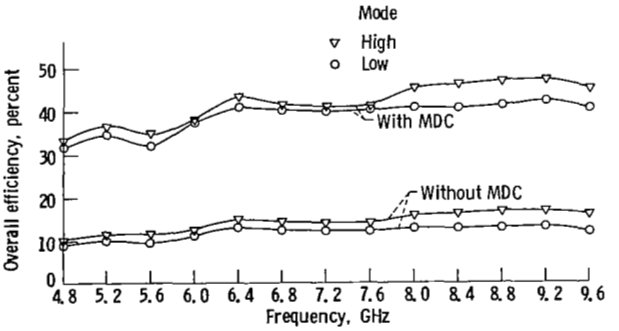


Figure 7. - Overall efficiency versus frequency at saturation.

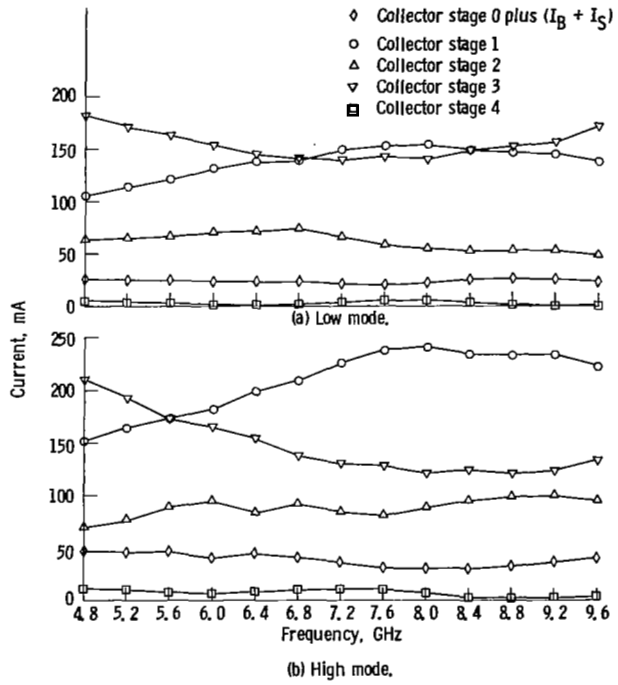


Figure 8. - MDC currents versus frequency at saturation (compromise optimization).

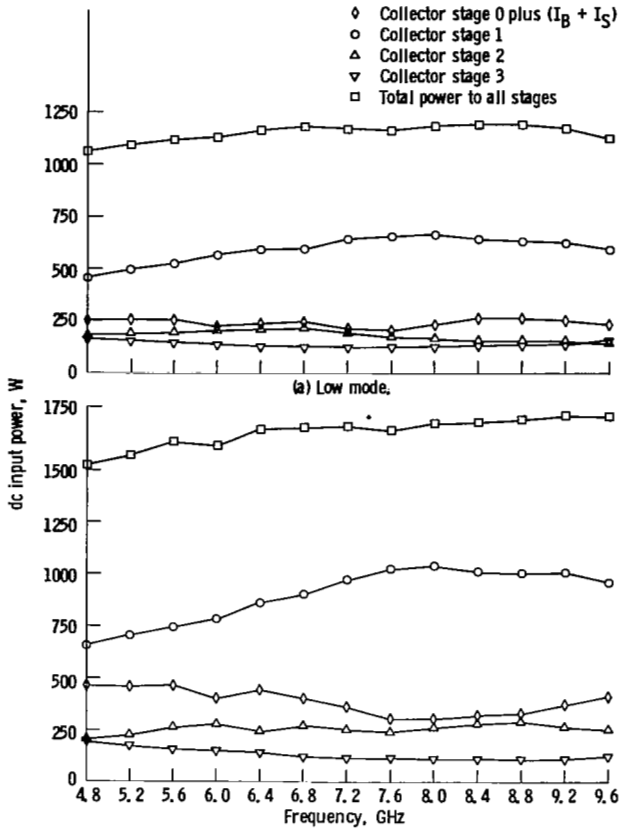


Figure 9. - dc power inputs versus frequency at saturation (compromise optimization).

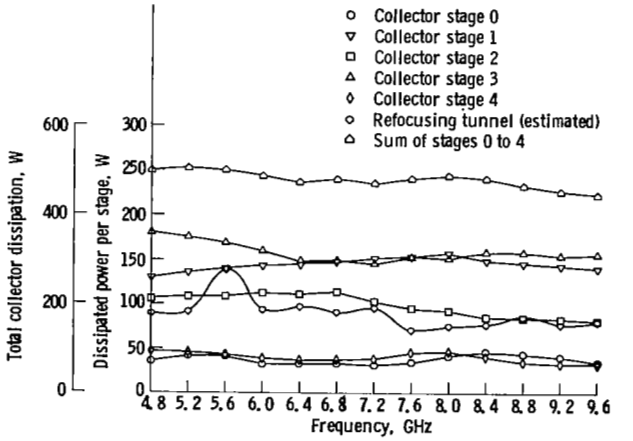


Figure 10. - Thermally dissipated power versus frequency - low mode at saturation (compromise optimization).

and 1.75 kilowatts for the low and high modes, respectively, as compared to 1.6 and 2.25 kilowatts for a production model TWT with a three-stage depressed collector tested at Lewis.

The thermal power dissipated on each of the collector electrodes and in the refocusing tunnel for the low mode as a function of frequency is shown in figure 10. The average dissipation for the high mode is smaller in all cases because of the reduced duty cycle.

The collector voltages (with respect to ground and normalized to $V_k$) used were 1.0, 0.91, 0.70, and 0.57.

*Single-mode CW TWT-MDC performance at saturation.*—In order to evaluate the TWT-MDC performance for single-mode operation, the MDC performance was optimized at or near the operating frequency producing maximum $P_{rf}$. Since this TWT is capable of considerably more rf output power than it generates at the nominal beam current in the low mode ($I_k = 0.38$ A), data were also obtained at beam currents of 0.4 and 0.42 ampere.

The rf output power as a function of frequency is shown in figure 11 for beam currents of 0.38, 0.4 and 0.42 ampere. The TWT-MDC performance is shown in figures 12 to 14. A very significant improvement in the overall efficiency was obtained. Collector efficiencies were in the range of 81 to 83 ½ percent.

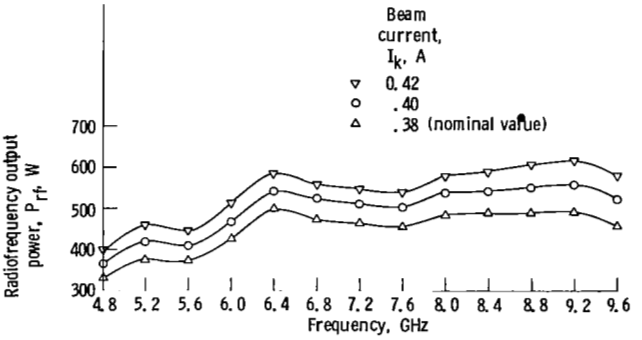


Figure 11. - Radiofrequency output power $P_{rf}$ versus frequency at saturation.

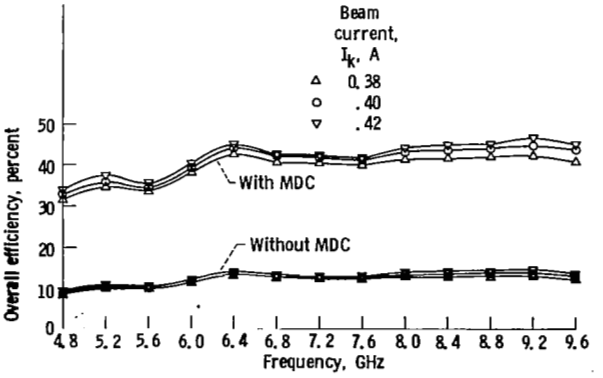


Figure 12. - Overall efficiency versus frequency at saturation.

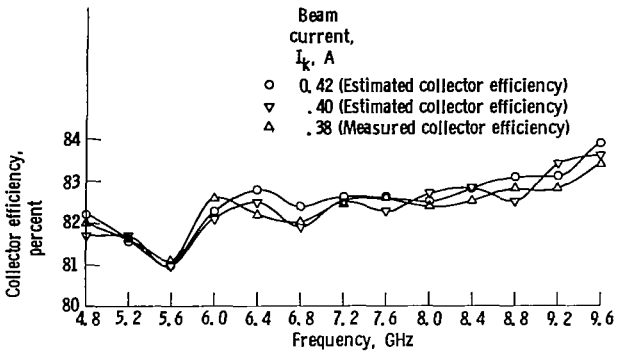


Figure 13. - Estimated and measured collector efficiencies versus frequency at saturation.

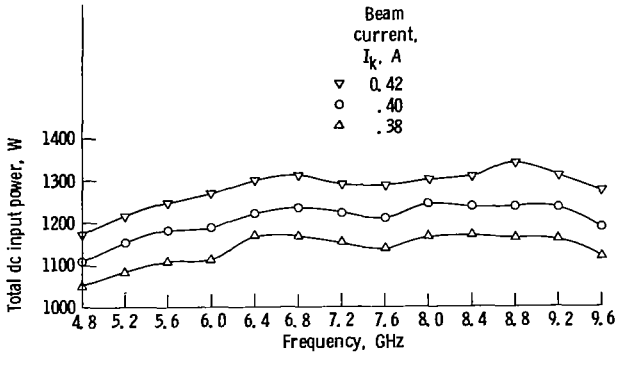


Figure 14. - Total dc input power versus frequency at saturation.

The average results across the octave bandwidth were

| Beam current, A | Overall efficiency | | Collector efficiency |
|---|---|---|---|
| | Without MDC | With MDC | |
| 0.38 | 11.9 | 39.3 | 82.3 |
| .40 | 12.4 | 41.1 | 82.5* |
| .42 | 12.9 | 42.1 | 82.4* |

*Estimated.

The collector stage currents and dc input power to the various stages as a function of frequency are shown in figures 15 and 16, respectively, for a cathode current of 0.42 ampere. The thermal powers dissipated on the collector stages are shown in figure 17.

The collector and overall efficiencies obtained for operation of this TWT-MDC at and below saturation at 9.2 gigahertz (for the same fixed set of MDC and refocusing system operating conditions) are shown in figure 18. The collector stage currents and dc input power to the various stages as a function of rf output power are shown in figures 19 and 20, respectively. The thermal power dissipated on the collector stages as a function of rf output power at

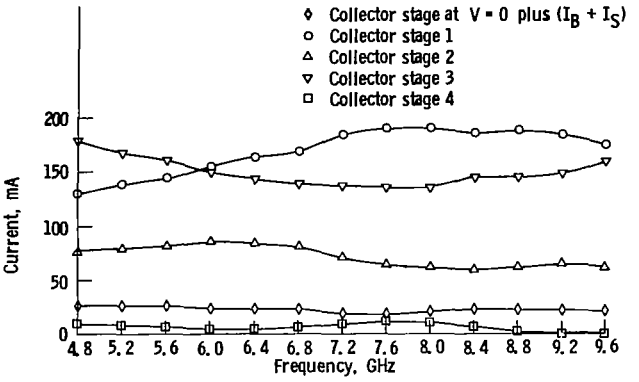


Figure 15. - Collector stage current versus frequency for saturation at 9.2 gigahertz and $I_k$ = 0.42 ampere.

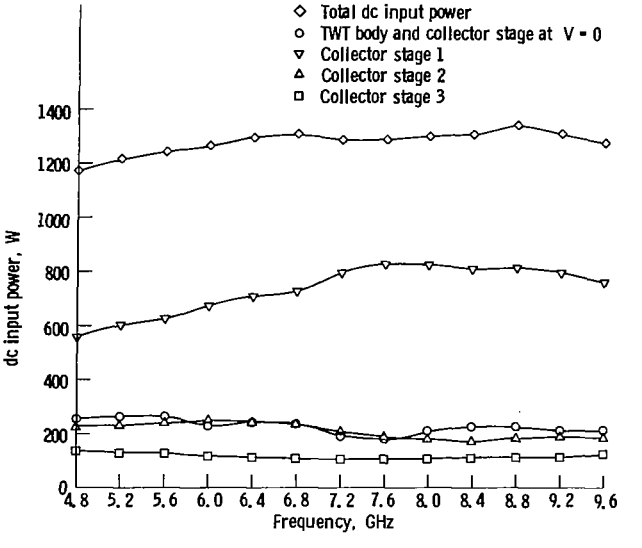


Figure 16. - dc input power per stage versus frequency for saturation at 9.2 gigahertz and $I_k$ = 0.42 ampere.

9.2 gigahertz is shown in figure 21. Maximum thermal dissipation and maximum dc input power to several of the collector stages occurred far below saturation.

The collector stage voltages (with respect to ground and normalized to $V_k$) used were 1.0, 0.92, 0.70 and 0.56. Similar results and trends were obtained at beam currents of 0.38 and 0.40 ampere.

*Dual-mode TWT-MDC performance for a 10:1 pulse-up in output power.*—For certain applications, both in ECM and communications, a large (up to 10:1) pulse-up capability in output power is required. The approach commonly used to achieve this is to pulse up the beam current. Typically, beam current pulse-up ratios (over the low mode) of 3 to 5 have been considered for a 10:1 pulse-up in output power. However, this introduces some severe problems in

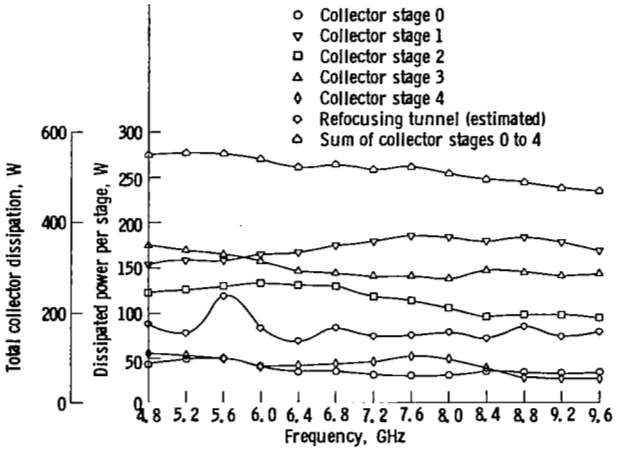


Figure 17. - Thermal power dissipated on collector stages versus frequency at saturation and $I_k$ = 0.42 ampere.

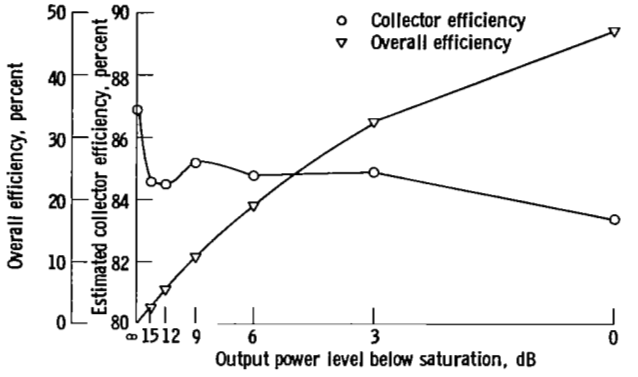


Figure 18. - Collector and overall efficiencies versus output power level below saturation at 9.2 gigahertz and $I_k$ = 0.42 ampere.

the areas of beam optics and control (especially for PPM focused TWT's) and in TWT circuit design since a number of important TWT parameters are functions of the beam current and effective beam radius.

The required pulse-up beam current can be significantly reduced, and the associated problems mitigated, if the low mode can represent operation of the TWT well below saturation. This alternative approach is practical only if an extremely efficient depressed collector for the low mode can be used to ensure a reasonable TWT overall efficiency. The problem of developing such a collector, however, is compounded by the fact that the collector operation cannot be optimized for the low mode: Extreme collector depression for the low mode (well below saturation) can produce a disastrous amount of backstreaming to the TWT in the pulsed-up mode and subsequent TWT failure. Therefore, the MDC optimization involves a compromise between the two

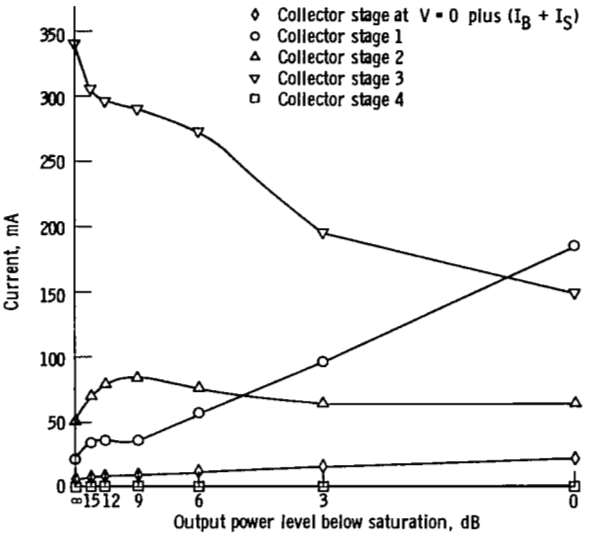


Figure 19. - Collector stage currents versus output power level at 9.2 gigahertz and $I_k$ = 0.42 ampere.

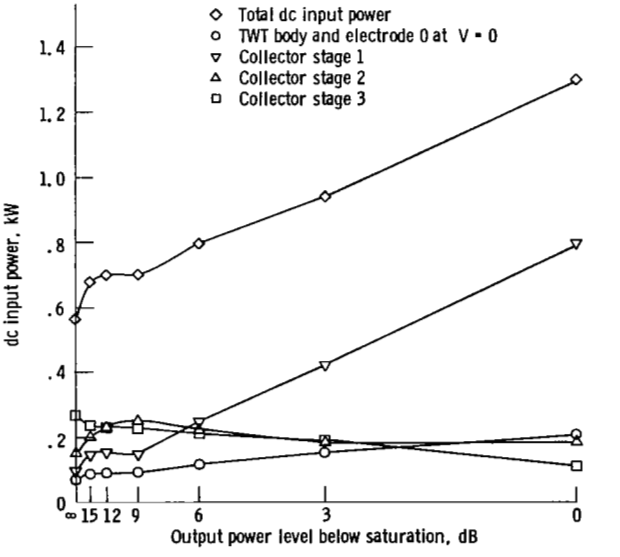


Figure 20. - dc input power versus output power level below saturation at 9.2 gigahertz and $I_k$ = 0.42 ampere.

operating modes.

In order to evaluate the effectiveness of this type of MDC for a fixed set of operating conditions over a 10:1 pulse-up range, where the high mode represents saturated operation (the most difficult case) and the low mode cw operation well below saturation (8 dB for this TWT), the dual-mode TWT was operated over the range of output powers of 81 to 810 watts. The compromise collector optimizations performed favored the low (cw) mode since the high (pulsed-up)

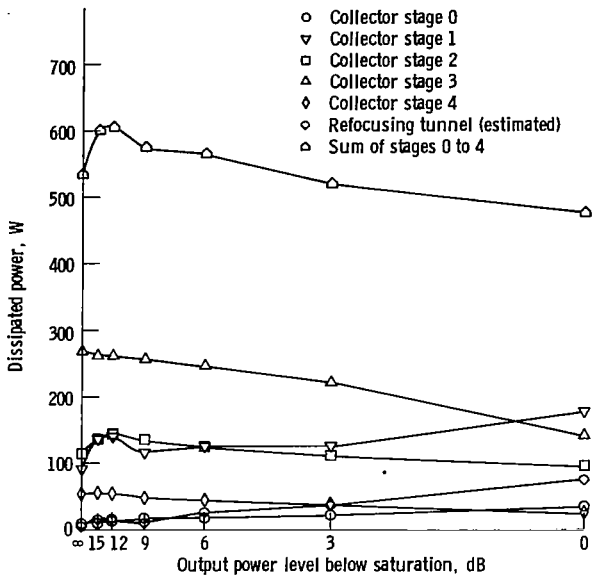


Figure 21. - Thermally dissipated power versus output power level below saturation at 9.2 gigahertz and $I_k$ = 0.42 ampere.

TABLE II.—DUAL-MODE TWT-MDC PERFORMANCE AT AND BELOW SATURATION FOR A FIXED SET OF MDC AND REFOCUSING SYSTEM OPERATING CONDITIONS (9.2 GHz)

| Mode | Pulse-up ratio | Overall efficiency | | Collector efficiency, percent |
|---|---|---|---|---|
| | | Without MDC | With MDC | |
| High | 1.0 (Saturation) | 16.7 | 41.7 | 76.2 |
| Low | 1.6 (Saturation) | 13.4 | 40.0 | 79.6 |
| | 2 | 10.8 | 37.0 | 81.7 |
| | 3 | 7.2 | 31.3 | 84.5 |
| | 4 | 5.4 | 26.9 | 85.9 |
| | 5 | 4.3 | 23.4 | 86.6 |
| | 6 | 3.6 | 20.9 | 87.2 |
| | 7 | 3.1 | 18.6 | 87.1 |
| | 8 | 2.6 | 16.6 | 87.4 |
| | 9 | 2.4 | 15.3 | 87.6 |
| | 10 | 2.1 | 14.2 | 87.7 |
| | 16 (10:1 in low mode | 1.3 | 10.0 | 88.8 |
| | 20 | 1.1 | 8.6 | 89.2 |
| | DC beam | ---- | ---- | 91.3 |

mode often represents a very low duty-cycle application. Data were also taken at other levels of output power (including saturation in the low mode and 10 dB below saturation in the low mode) for this fixed set of MDC and refocusing system operating conditions. The results are compiled in table II and in figure 22. The data are plotted for both 2 mode operation (the power is compared to $P_{rf}$ saturation for the high mode) and for the low mode only (compared to $P_{rf}$ saturation in the low mode). A

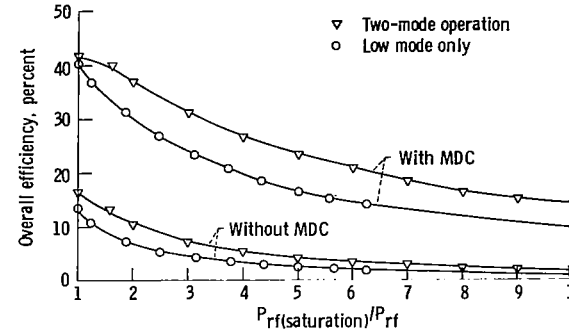


Figure 22. - Overall efficiency versus output power level below saturation for fixed set of MDC operating conditions at 9.2 gigahertz.

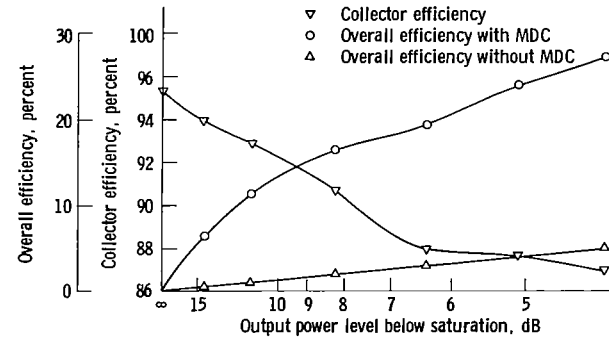


Figure 23. - TWT overall and collector efficiencies versus output power level below saturation. Linear range of low mode at 6.4 gigahertz and $I_k$ = 0.38 ampere.

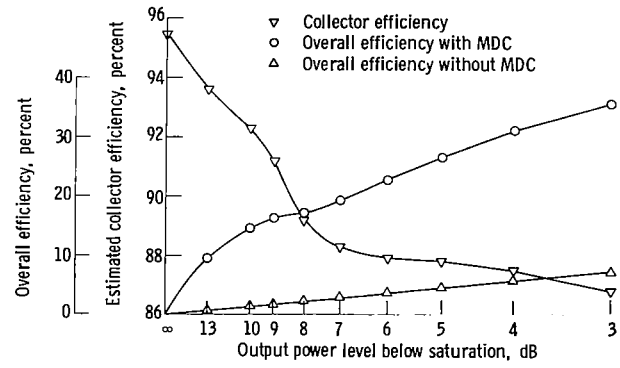


Figure 24. - TWT overall and MDC efficiencies versus output power level below saturation. Linear range of low mode at 9.2 gigahertz and $I_k$ = 0.42 ampere.

minimum efficiency of 14 percent was obtained for dual-mode operation over a 10:1 range in output power.

The collector voltages (with respect to ground and normalized to $V_k$) used were 1.0, 0.93, 0.84 and 0.57.

*TWT-MDC performance for operation of the TWT in the linear range.*—The TWT was operated

over its linear range in the low mode to simulate applications where the TWT must be operated at constant output power in the linear, low-distortion range and consequently at very low (a few percent) electronic efficiencies. The MDC performance was individually optimized at each TWT operating point.

The results are shown in figure 23 and 24 for frequencies of 6.4 and 9.2 gigahertz, respectively. At the low end of the linear range the collector efficiencies exceed 90 percent, leading to a very substantial improvement in the overall efficiency. Without the MDC the overall efficiency would be prohibitively low for many space and airborne applications.

Typical voltages (with respect to ground and normalized to $V_k$) used were 1.0, 0.95, 0.90, and 0.61.

## Concluding Remarks

A computer designed 2.4-centimeter-diameter four-stage depressed collector of fixed geometric design was optimized and evaluated over a wide range of TWT and MDC operating conditions. The combination of refocusing system and MDC proved to be highly adaptable to the wide range of TWT applications considered.

The high collector efficiencies achieved in combination with the relatively low fixed losses of this TWT sample enabled the following demonstrations:

1. Overall efficiencies in the range of 40 to 47 percent for both low and high modes at saturation over most of the octave bandwidth, and collector efficiencies in the range of 81 to 83 ½ percent.

2. A minimum overall efficiency of 14 percent for operation of the dual-mode TWT over a 10:1 range in output power.

3. Overall efficiencies as high as 35 percent for operation of the TWT in the linear range.

The 90 percent and greater collector efficiencies for the low end of the linear range make possible a number of new applications which would be impractical without the MDC. Significantly higher MDC efficiencies should be possible with individually optimized MDC geometric design for each, specific application.

Lewis Research Center
National Aeronautics and Space Administration
Cleveland, Ohio, February 3, 1981

## References

1. Kosmahl, Henry G.: A Novel, Axisymmetric, Electrostatic Collector for Linear Beam Microwave Tubes. NASA TN D-6093, 1971.
2. Kosmahl, Henry G.; and Ramins, Peter: Small-Size 81- to 83.5-Percent Efficient 2- and 4-Stage Depressed Collectors for Octave-Bandwidth High-Performance TWT's. IEEE Trans. Electron Devices, vol. ED-24, no. 1, Jan. 1977, pp. 36–44.
3. Kosmahl, Henry G.: An Electron Beam Controller. U.S. Patent 3,764,850, Oct. 1973.
4. Stankiewicz, N.: Analysis of Spent Beam Refocusing to Achieve Optimum Collector Efficiency. IEEE Trans. Electron Devices, vol. ED-24, no. 1, Jan. 1977, pp. 32–36.
5. Dayton, J. A., Jr.; et al.: Analytical Prediction with Multidimensional Computer Programs and Experimental Verification of the Performance, at a Variety of Operating Conditions, of Two Traveling Wave Tubes with Depressed Collectors. NASA TP-1449, 1979.
6. Dayton, J. A., Jr.; et al.: Analytical Prediction and Experimental Verification of the Performance, at a Variety of Operating Conditions, of a Dual-Mode Traveling Wave Tube with Multistage Depressed Collectors. NASA TP-1831, 1981.
7. Kosmahl, Henry G.: Comments on Measuring the Overall and the Depressed Collector Efficiency in TWT's and Klystron Amplifiers. IEEE Trans. Electron Devices, vol. ED-26, no. 2, Feb. 1979, p. 156.
8. Ramins, P.; and Fox, T. A.: Efficiency Enhancement of Octave-Bandwidth Traveling Wave Tubes by Use of Multistage Depressed Collectors. NASA TP-1416, 1979.
9. Gilmour, A. S., Jr.: Bakeable Ultra-High Vacuum Gate Valve for Microwave Tube Experimentation. J. Vac. Sci. Technol., vol. 13, no. 6, Nov.-Dec. 1976, pp. 1199–1201.
10. Ramins, P.; and Fox, T. A.: Multistage Depressed Collector with Efficiency of 90 to 94 Percent for Operation of a Dual-Mode Traveling Wave Tube in the Linear Region. NASA TP-1670, 1980.

| 1. Report No. | 2. Government Accession No. | 3. Recipient's Catalog No. |
|---|---|---|
| NASA TP-1832 | | |

| 4. Title and Subtitle | 5. Report Date |
|---|---|
| PERFORMANCE OF COMPUTER-DESIGNED SMALL-SIZED FOUR-STAGE DEPRESSED COLLECTOR FOR OPERATION OF DUAL-MODE TRAVELING WAVE TUBE | August 1981 |
| | 6. Performing Organization Code 506-61-32 |
| 7. Author(s) | 8. Performing Organization Report No. |
| Peter Ramins and Thomas A. Fox | E-643 |
| | 10. Work Unit No. |
| 9. Performing Organization Name and Address | |
| National Aeronautics and Space Administration<br>Lewis Research Center<br>Cleveland, Ohio 44135 | 11. Contract or Grant No. |
| | 13. Type of Report and Period Covered |
| 12. Sponsoring Agency Name and Address | Technical Paper |
| National Aeronautics and Space Administration<br>Washington, D.C. 20546 | 14. Sponsoring Agency Code |

15. Supplementary Notes

16. Abstract

A computer-designed axisymmetric 2.4-cm-diameter four-stage depressed collector was evaluated in conjunction with an octave bandwidth, dual-mode traveling wave tube (TWT). The TWT was operated over a wide range of conditions to simulate different applications. The collector performance was optimized (within the constraint of fixed collector geometry which was designed for operation of the TWT at saturation) over the range of TWT operating conditions covered. For operation of the dual-mode TWT at saturation, average collector efficiencies of 81 1/2 and 82 percent for the high and low modes, respectively, were obtained across an octave bandwidth, leading to a three-fold increase in the TWT overall efficiency. For operation of the TWT in the linear, low distortion range, collector efficiencies of 87 to 92 percent were obtained, leading to TWT overall efficiencies as high as 35 percent. For operation of the dual-mode TWT over a 10 to 1 range in output power, overall efficiencies of 14 to 41 percent were obtained.

| 17. Key Words (Suggested by Author(s)) | 18. Distribution Statement |
|---|---|
| Traveling wave tube<br>Multistage depressed collector | Unclassified - unlimited<br>STAR Category 33 |

| 19. Security Classif. (of this report) | 20. Security Classif. (of this page) | 21. No. of Pages | 22. Price* |
|---|---|---|---|
| Unclassified | Unclassified | 13 | A02 |

* For sale by the National Technical Information Service, Springfield, Virginia 22161

NASA-Langley, 1981